



Fermi National Accelerator Laboratory

FERMILAB-FN-610

MUSIM
Program to Simulate Production and Transport of Muons
in Bulk Matter
ERRATUM

A. Van Ginneken

Fermi National Accelerator Laboratory
P.O. Box 500, Batavia, Illinois 60510

September 1993

Disclaimer

This report was prepared as an account of work sponsored by an agency of the United States Government. Neither the United States Government nor any agency thereof, nor any of their employees, makes any warranty, express or implied, or assumes any legal liability or responsibility for the accuracy, completeness, or usefulness of any information, apparatus, product, or process disclosed, or represents that its use would not infringe privately owned rights. Reference herein to any specific commercial product, process, or service by trade name, trademark, manufacturer, or otherwise, does not necessarily constitute or imply its endorsement, recommendation, or favoring by the United States Government or any agency thereof. The views and opinions of authors expressed herein do not necessarily state or reflect those of the United States Government or any agency thereof.

MUSIM
Program to Simulate Production and Transport of
Muons in Bulk Matter
ERRATUM

A. Van Ginneken
Fermi National Accelerator Laboratory*
P. O. Box 500, Batavia, IL 60510

September 1993

An error discovered in the program MUSIM requires the results included in [1] to be restated. Single Coulomb scattering—treated as a correction to multiple scattering—is not properly damped by form factors in the results presented in [1]. This causes excessive large angle scattering and hence increased radial excursions of the muons. Ref. [1] also includes some results of the program CASIMU for comparison. In older versions of this program the single scattering correction was absent. However for [1] both programs relied on the same muon transport. A revised muon scattering routine is briefly described below and corrected results obtained with it are presented.

Multiple Scattering

In the usual formulation [2, 3] of multiple scattering the projected angles follow a Gaussian distribution with $\sigma = \theta_s/\sqrt{2}$. This is equivalent to the square of the spatial angle being exponentially distributed, i.e.,

$$P(\theta^2) = \theta_s^{-2} \exp(-\theta^2/\theta_s^2) \quad (1)$$

with

$$\theta_s = (0.0212/\beta p) \sqrt{\ell/X_0} \quad (2)$$

*Work supported by the U.S. Department of Energy under contract No. DE-AC02-76CHO3000.

where $\beta = v/c$ as usual, p is the momentum in GeV/c , ℓ the steplength, and X_0 the radiation length of the material.

Coherent Single Scattering

The probability for single scattering off the entire nucleus is taken as the usual Rutherford scattering of two point particles multiplied by a *nuclear* form factor. The former may be expressed as [3]

$$P(\eta)d\eta = \frac{1}{2 \ln(210Z^{-1/3})} \frac{d\eta}{\eta^3} \quad (3)$$

where $\eta = \theta/\theta_s$ [4]. Equivalently

$$P(\eta^2)d\eta^2 = \frac{1}{4 \ln(210Z^{-1/3})} \frac{d\eta^2}{(\eta^2)^2}. \quad (4)$$

In eqs. 3 and 4 the dependence on steplength is contained in θ_s , which enters via the definition of η . In [3] it is shown that multiple scattering dominates when $\eta < 2$ and to good approximation one may simply add single scattering above $\eta = 2$ to the complete Gaussian of multiple scattering for that step. From eq. 3 or 4 the total probability for single scattering is

$$P(\eta > 2) = \frac{1}{16 \ln(210Z^{-1/3})} \quad (5)$$

independent of ℓ . The form factor is chosen for simplicity as

$$F_N = (1 + t/d)^2 \quad (6)$$

from ref. [5], where t is the square of the 4-momentum transfer and $d = 0.164A^{-2/3}$ in GeV^2 .

Incoherent Single Scattering

For incoherent scattering, it is assumed that the differential cross section is that of single μp scattering, multiplied by the *proton* form factor and a Pauli suppression factor which takes into account that a proton cannot transfer to an already occupied state as a result of the collision. Again, events with angle below $2\theta_s$ are neglected compared to multiple scattering. The differential scattering cross section is

$$d\sigma/dt = 4\pi Z(\alpha/t)^2 \quad (7)$$

per nucleus. For angles above $2\theta_c$, this leads to a total cross section

$$\sigma_{tot} = 4\pi\alpha^2/t_{min} \quad (8)$$

where $t_{min} = 4p^2\theta_c^2$. The probability for such a scattering is

$$P(t > t_{min}) = N_{Av}\rho\sigma_{tot}\ell/A \quad (9)$$

in a step of length ℓ . By use of eq. 2 σ_{tot} may be rewritten as

$$\sigma_{tot} = 0.145ZX_0/\ell \quad (10)$$

in millibarns which, upon substitution in eq. 9, yields

$$P(t > t_{min}) = 8.71 \cdot 10^{-5} X_0\rho Z/A \quad (11)$$

again independent of ℓ . This is to be multiplied by the product of the proton form factor and the Pauli suppression factor. Again from ref. [5]:

$$F_p = \frac{1 + 7.78\tau}{(1 + \tau)(1 + t/0.71)^4} \quad (12)$$

is the form factor with $\tau = t/4m_p^2$. The suppression factor is unity for $Q \geq 2P_F$ where $Q = \sqrt{t\tau + t}$ is the recoil proton momentum and $P_F = 0.25$ GeV the Fermi momentum. For $Q < 2P_F$:

$$C(Q) = (3Q/4P_F) \left[1 - (1/12)(Q/P_F)^2 \right]. \quad (13)$$

Nuclear shadowing is ignored but the effect should be relatively small because of the larger angles and because it pertains to protons only.

Scattering Algorithm

For each step during muon transport the mean square angle for multiple scattering is obtained and a random (squared) angle is then selected from eq. 1. It is then determined if coherent scattering ($\theta > 2\sigma$) occurred during this step with a probability based on the cross section without form factor (and thus overestimated). If so, another (squared) angle is selected from the single scattering distribution and the form factor corresponding to this angle is evaluated. A uniform random number is compared with the form factor: if less the scattering event is accepted, otherwise no scattering takes place—thereby correcting the overestimated probability [6]. An entirely

similar procedure follows for incoherent scattering. In addition, there may be angular deflections from bremsstrahlung, direct e^+e^- production, nuclear interaction, and δ -ray production as determined elsewhere in the program. The squares of these individual angles are summed to obtain a new direction for the μ . The recoil kinetic energy of nucleus or proton is subtracted from that of the muon.

Corrected Results

Figs. 1–10 show results obtained with the corrected code which replace figure-for-figure those in [1]. Because of lesser excursions the radial scale is reduced to 10 m (from 15 m). An effort is made to treat the low z –low r region more accurately by keeping a separate tally over a finer array in that vicinity. The largest effects of correcting the error are clearly in the low z –high r region. On-axis longitudinal penetration—crucial in many applications—is little affected.

Acknowledgement. My apologies for this error and and my thanks to C. Bhat and P. Martin for their questions about some MUSIM results.

References

- [1] A. Van Ginneken, Fermilab Report FN-594 (1992).
- [2] B. Rossi, *High Energy Particles*, Prentice-Hall, Englewood Cliffs, N.J., 1952, pp. 63ff.
- [3] J. D. Jackson, *Classical Electrodynamics*, 2nd ed., J. Wiley, New York, 1975, pp. 450ff.
- [4] The expression differs from the one in [3] because eq. 3 refers to the spatial—not the projected—angle.
- [5] Y.-S. Tsai, *Rev. Mod. Phys.* **46**, 815 (1974).
- [6] To better explore large radial excursions the procedure is modified to increase large angle scattering but with a compensating reduction in weight.

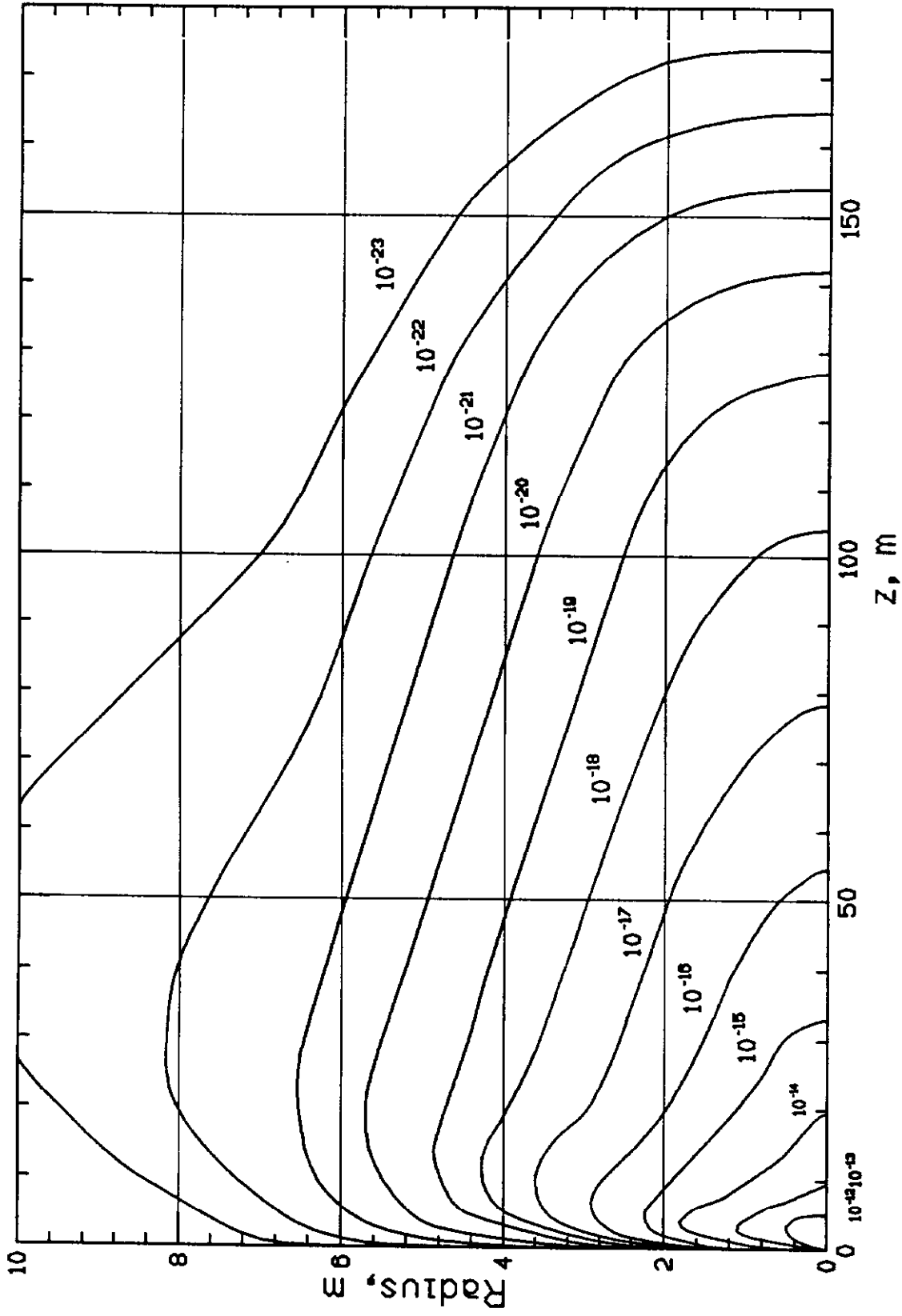


Fig. 1 Isodose contours due to muons in rad/inc.proton for 0.1 TeV protons incident on homogeneous soil as calculated by MUSIM.

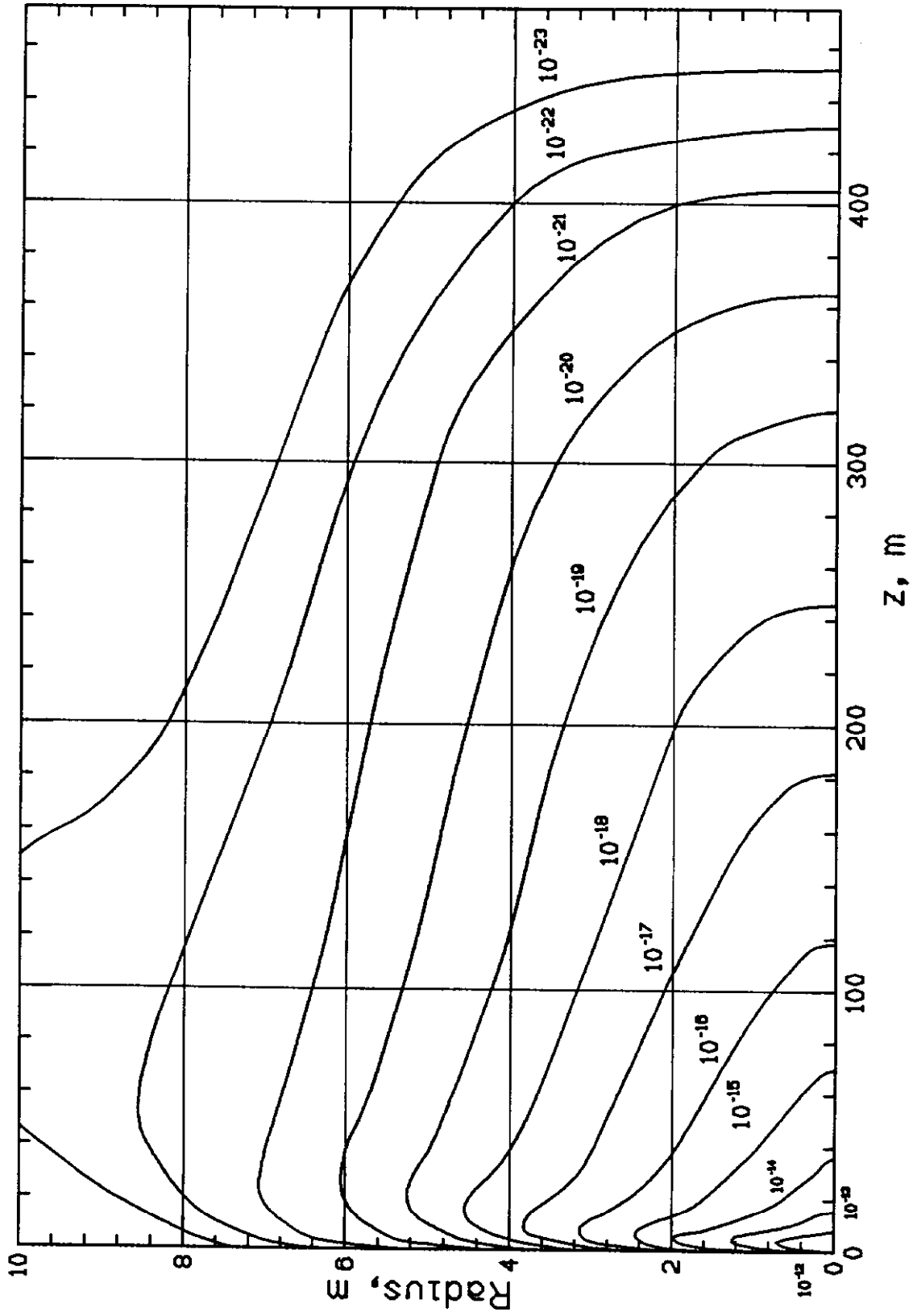


Fig. 2 Isodose contours due to muons in rad/inc.proton for 0.3 TeV protons incident on homogeneous soil as calculated by MUSIM.

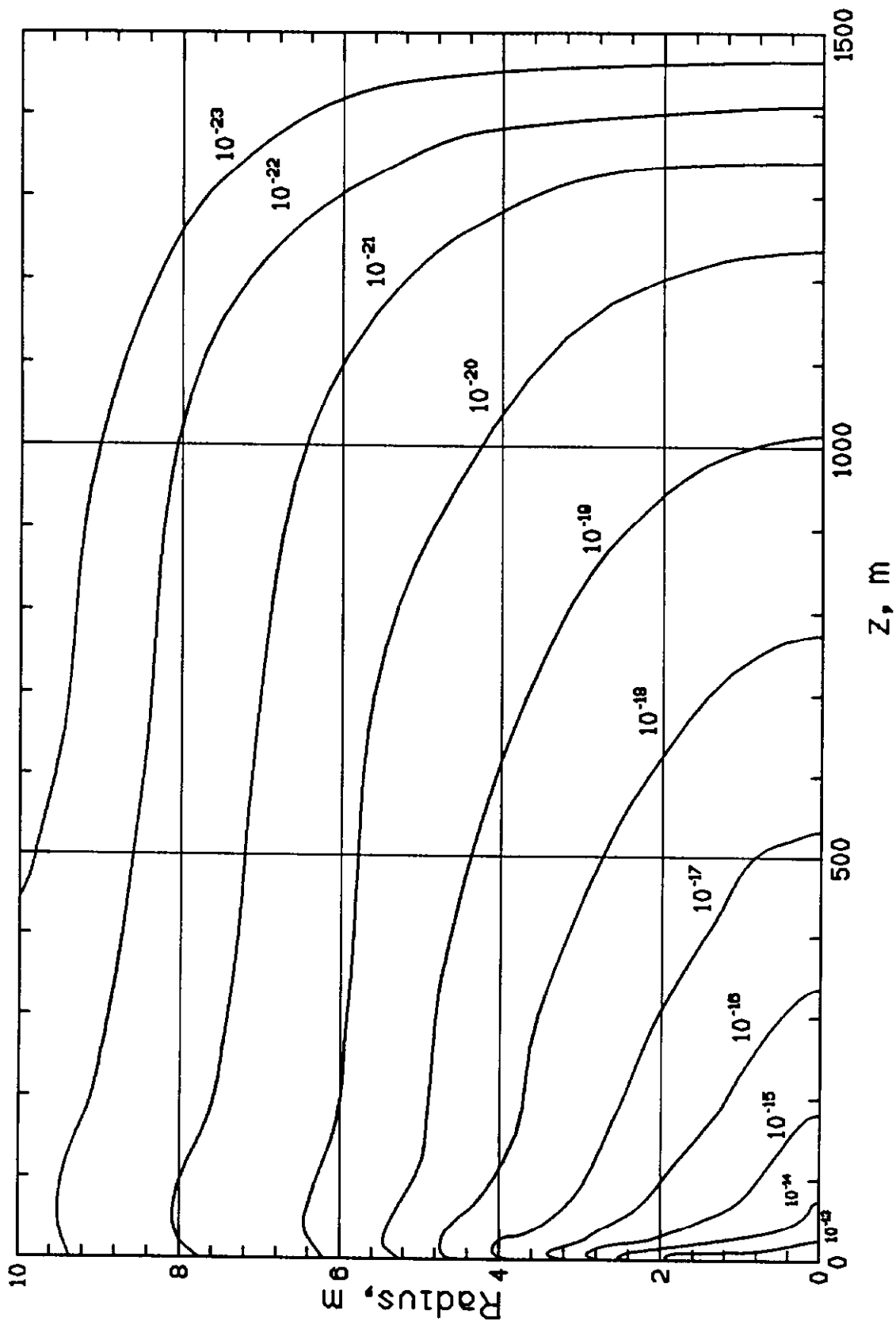


Fig. 3 Isodose contours due to muons in rad/inc.proton for 1 TeV protons incident on homogeneous soil as calculated by MUSIM.

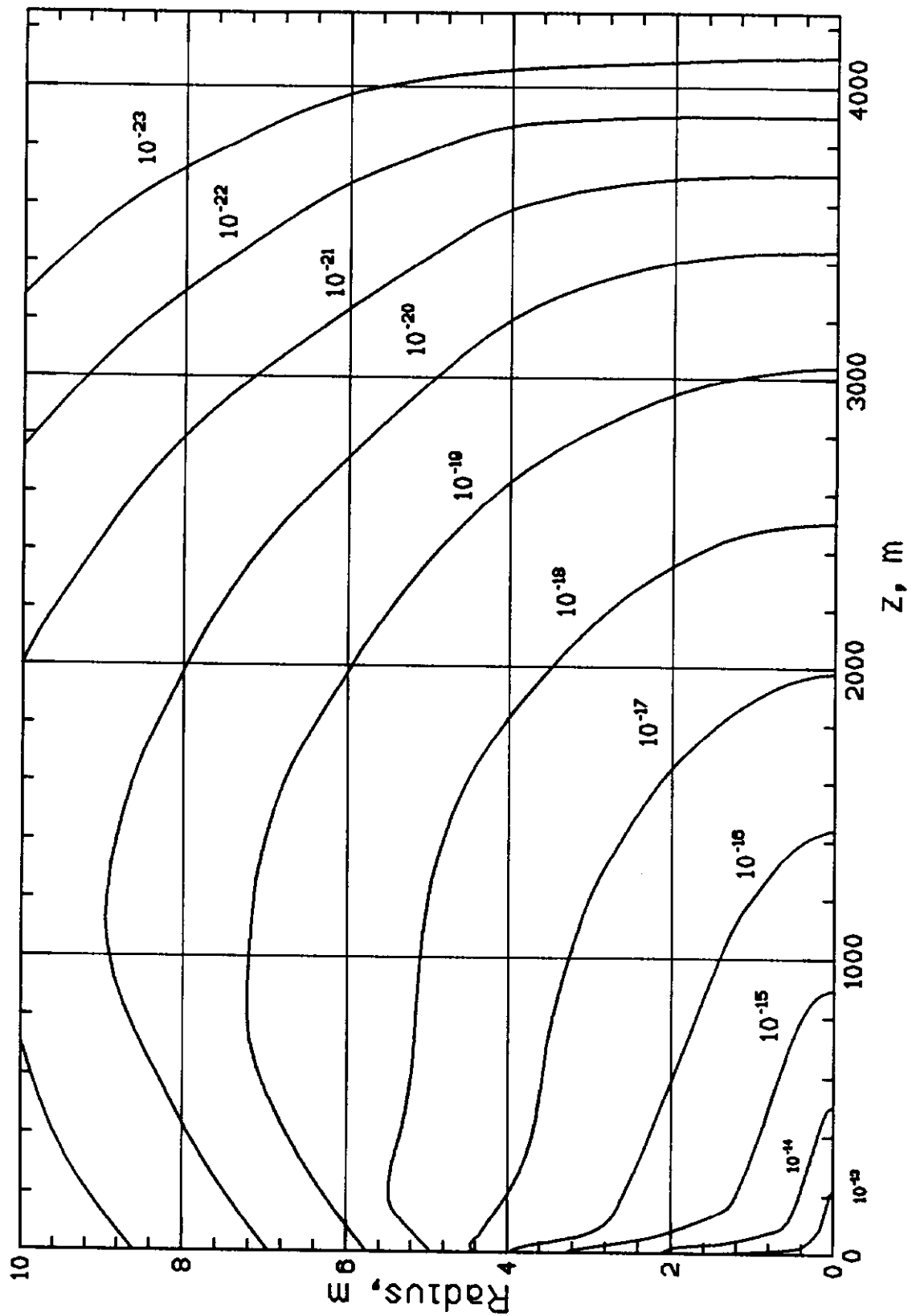


Fig. 4 Isodose contours due to muons in rad/inc.proton for 8 TeV protons incident on homogeneous soil as calculated by MUSIM.

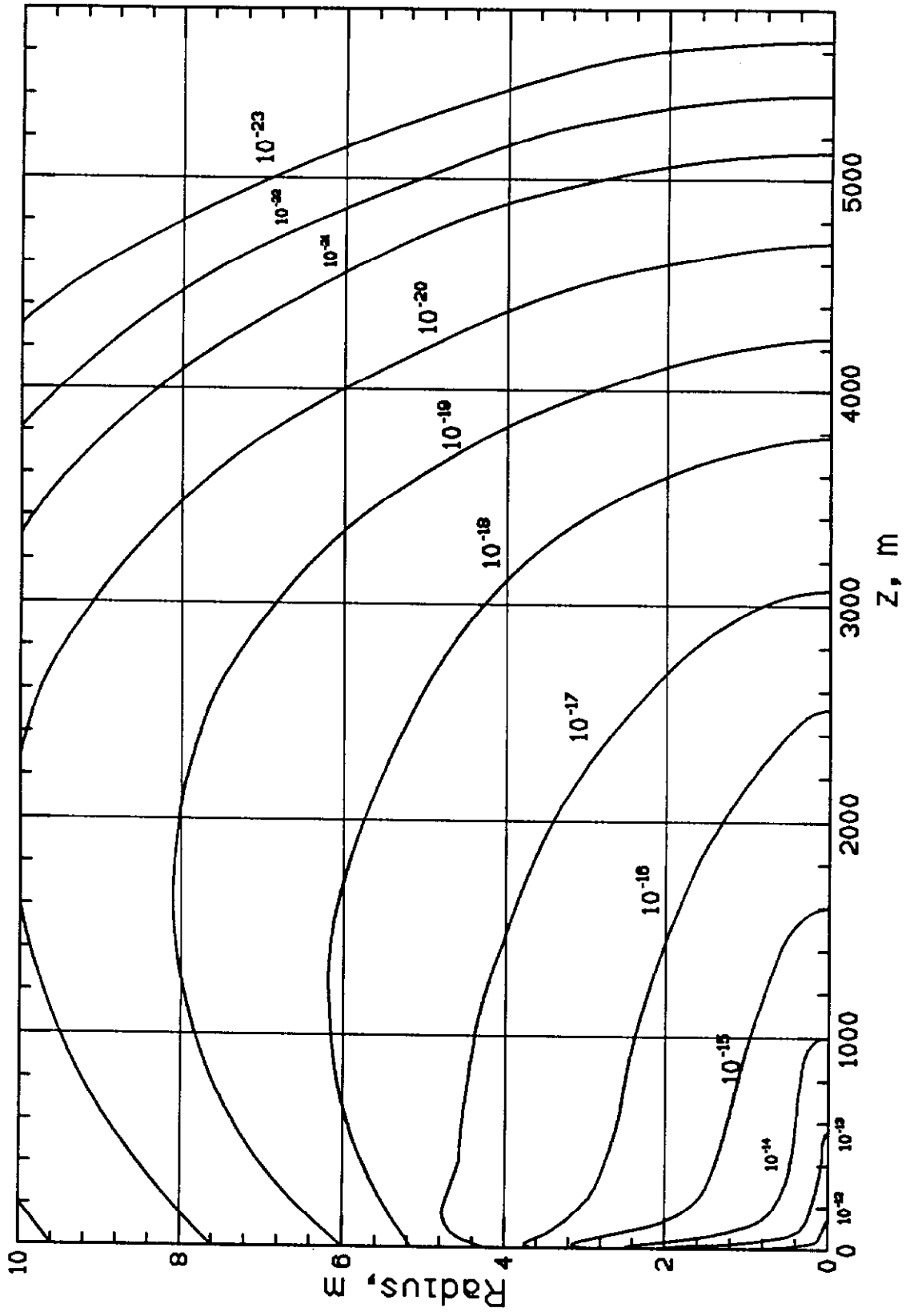


Fig. 5 Isodose contours due to muons in rad/inc.proton for 20 TeV protons incident on homogeneous soil as calculated by MUSIM.

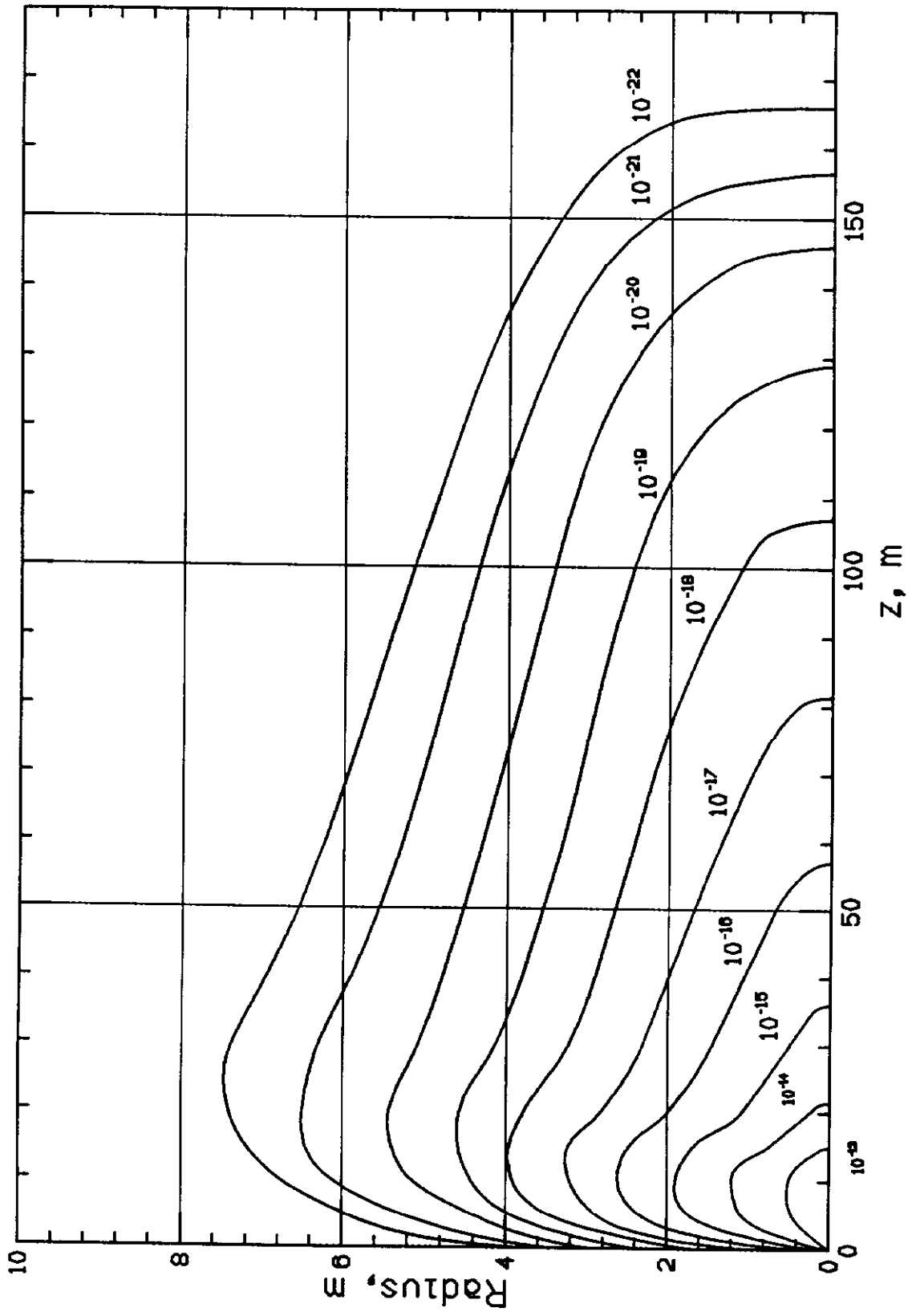


Fig. 6 Isodose contours due to muons in rad/inc.proton for 0.1 TeV protons incident on homogeneous soil as calculated by CASIMU.

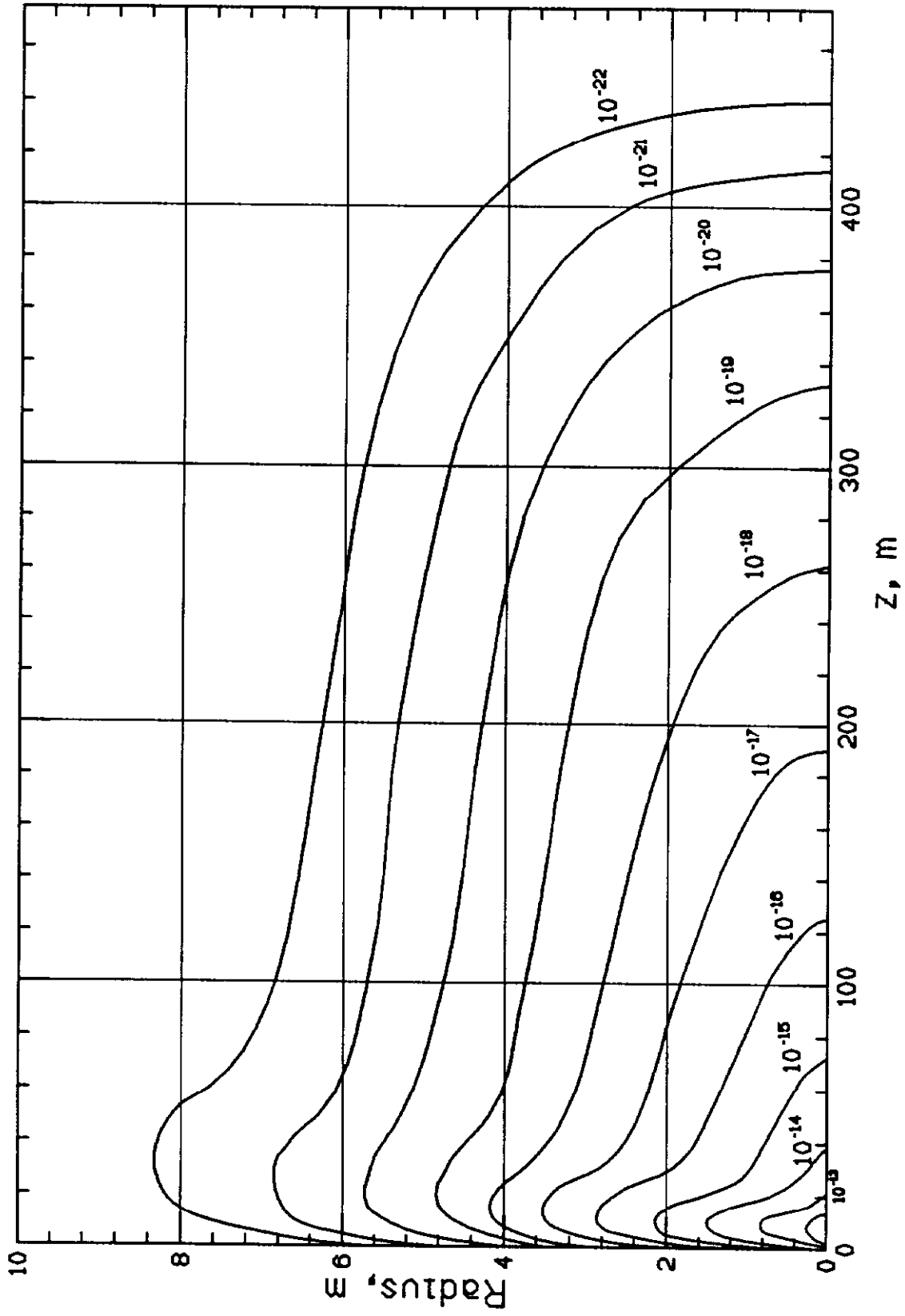


Fig. 7 Isodose contours due to muons in rad/inc.proton for 0.3 TeV protons incident on homogeneous soil as calculated by CASIMU.

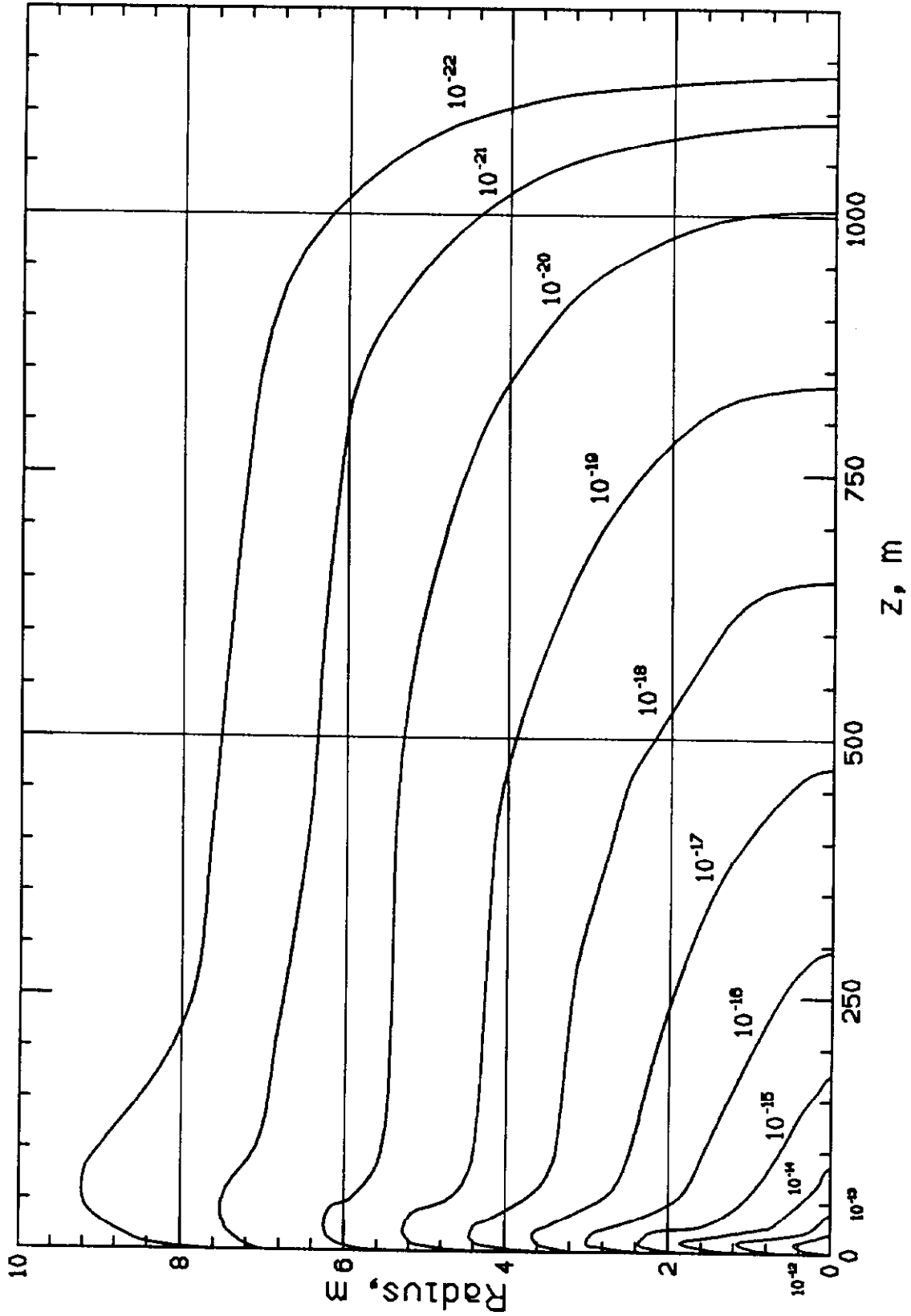


Fig. 8 Isodose contours due to muons in rad/inc.proton for 1 TeV protons incident on homogeneous soil as calculated by CASIMU.

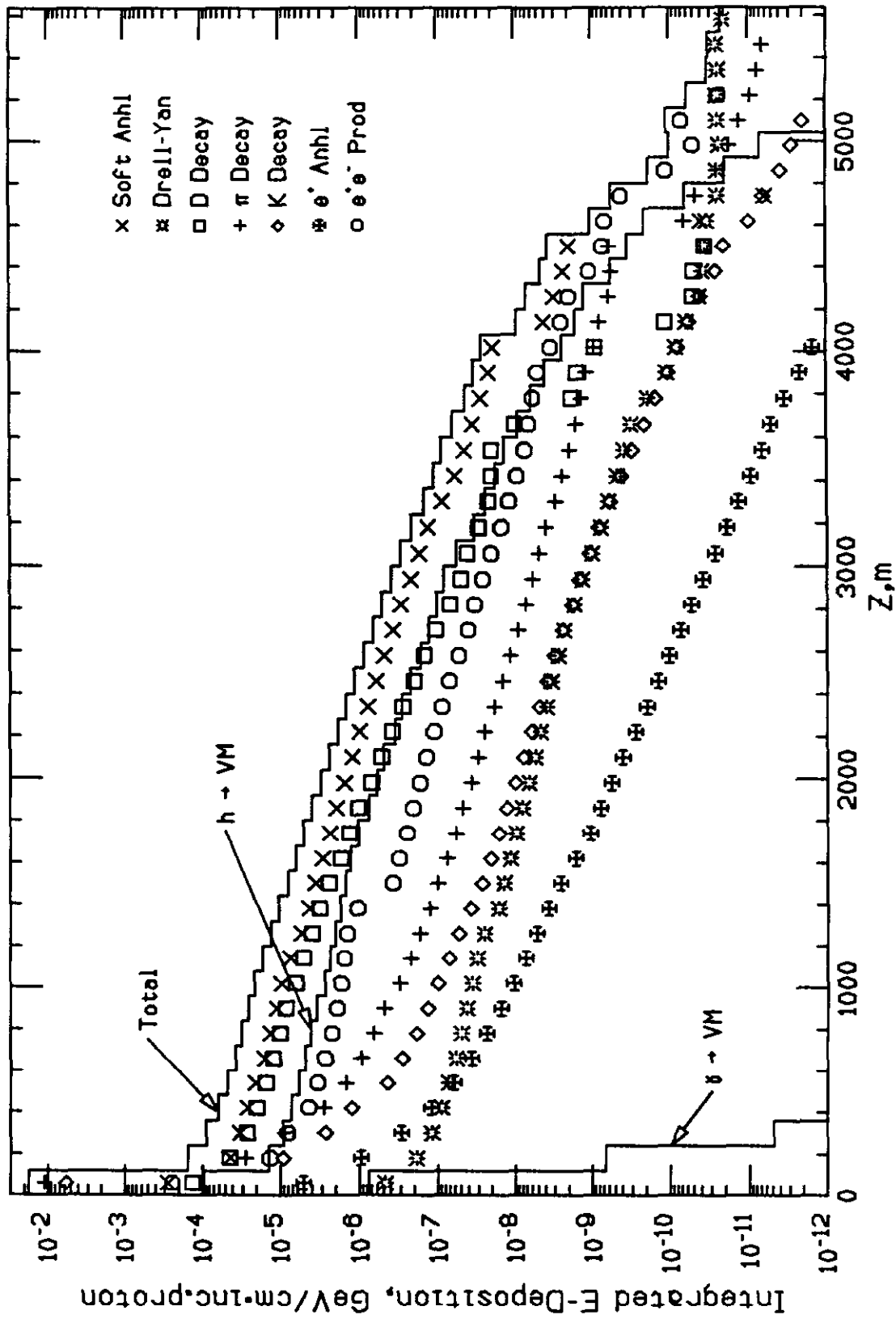


Fig. 9 Radially integrated muon energy deposition by production mechanism as a function of longitudinal distance for 20 TeV protons incident on homogeneous soil as calculated by MUSIM.

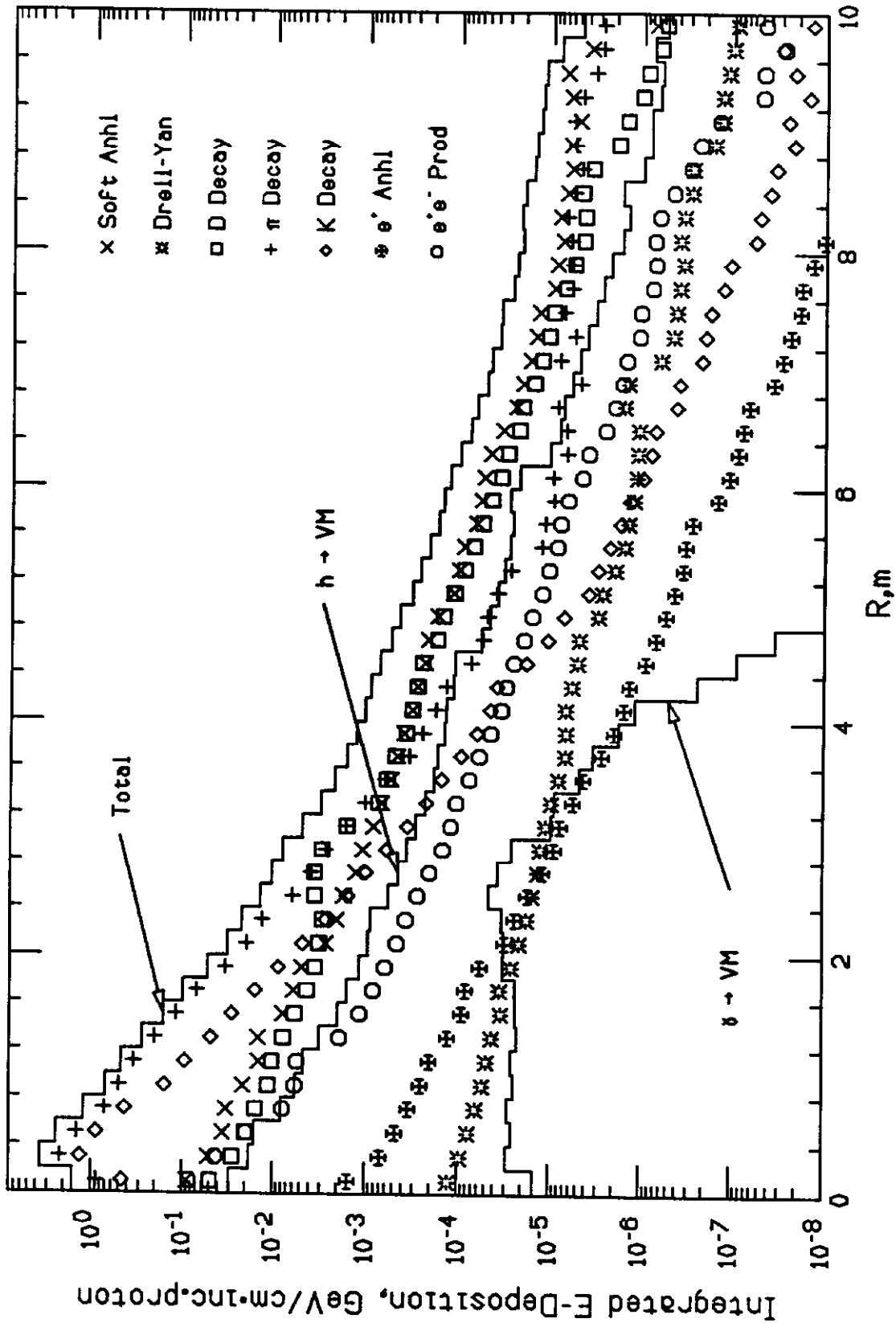


Fig. 10 Longitudinally integrated muon energy deposition by production mechanism as a function of radial distance for 20 TeV protons incident on homogeneous soil as calculated by MUSIM.